



Article

Adsorption of Multi-Collector on Long-Flame Coal Surface via Density Functional Theory Calculation and Molecular Dynamics Simulation

Gan Cheng ^{1,2,3,4,*} , Yujie Peng ¹, Yang Lu ¹  and Mengni Zhang ¹

- ¹ College of Chemistry and Chemical Engineering, Henan Polytechnic University, Jiaozuo 454003, China
² Henan Key Laboratory for Green and Efficient Mining & Comprehensive Utilization of Mineral Resources, Henan Polytechnic University, Jiaozuo 454003, China
³ State Environmental Protection Key Laboratory of Mineral Metallurgical Resources Utilization and Pollution Control, Wuhan University of Science and Technology, Wuhan 430081, China
⁴ Collaborative Innovation Center of Coal Work Safety and Clean High Efficiency Utilization, Henan Polytechnic University, Jiaozuo 454003, China
* Correspondence: chenggan464@126.com

Abstract: The quantum chemical properties of long-flame coal (LFC) and collectors (kerosene, diesel, diethyl phthalate (DEP), biodiesel collector (BDC), and emulsified biodiesel collector (EBDC)) were analyzed via the density functional theory (DFT). The molecular dynamics (MD) of the coal–collector–water system and the adsorption of collectors on LFC were conducted based on the first principles. The results showed that the frontier molecular orbitals of kerosene, diesel, DEP, and BDC were 0.38 eV, 0.28 eV, 0.27 eV, and 0.20 eV, respectively. The chemical reactivity order of the above mentioned collectors was BDC > DEP > diesel > kerosene. Kerosene, diesel, and DEP adsorbed with carbonyl, hydroxyl, and carboxyl groups in LFC, respectively. Carboxyl groups in BDC and carboxyl groups in LFC bilaterally adsorbed, while BDC repelled water molecules via hydrogen bonds on the LFC surface. In the systems of BDC and EBDC, the diffusion coefficients of a water molecule were $2.83 \times 10^{-4} \text{ cm}^2/\text{s}$ and $3.73 \times 10^{-4} \text{ cm}^2/\text{s}$. The emulsifier that adsorbed onto the oil–water interface of the coal–BDC–water system improved the dispersion of BDC during flotation, while at the same time increasing the number of hydrogen bonds between BDC and LFC, which accelerated the migration of water molecules from the LFC surface.

Keywords: long-flame coal; collector; quantum chemistry; molecular dynamics; adsorption



Citation: Cheng, G.; Peng, Y.; Lu, Y.; Zhang, M. Adsorption of Multi-Collector on Long-Flame Coal Surface via Density Functional Theory Calculation and Molecular Dynamics Simulation. *Processes* **2023**, *11*, 2775. <https://doi.org/10.3390/pr11092775>

Academic Editor: Hui Li

Received: 28 August 2023

Revised: 14 September 2023

Accepted: 15 September 2023

Published: 17 September 2023



Copyright: © 2023 by the authors. Licensee MDPI, Basel, Switzerland. This article is an open access article distributed under the terms and conditions of the Creative Commons Attribution (CC BY) license (<https://creativecommons.org/licenses/by/4.0/>).

1. Introduction

There is an abundant amount of low-rank coal (LRC) reserves, which account for 55% of total coal resources and are widely used in China [1,2]. Since China proposed its “30–60” goal to achieve peak carbon emission by 2030 and carbon neutrality by 2060, the clean and efficient utilization of LRC has become more significant [3,4]. LRC is characterized by its low metamorphism and carbon content, high moisture and volatile content. In order to meet the sustainability needs of energy conservation and emission reduction, it is, therefore, imperative to improve the quality of LRC [5,6]. Flotation is a promising method to improve the quality of LRC. Reagents are necessary during the flotation process. As one of the important reagents, collector can selectively adsorb on the surface of minerals and change the hydrophobicity of mineral surfaces; hydrophobic particles are easier to adhere on bubbles. The LRC surface is rich in oxygen-containing functional groups (–COOH, –OH, C–O–C, C=O, etc.), thereby easily forming hydrogen bonds with water molecules [7]. This causes difficulty for kerosene and diesel collectors to adsorb on the LRC surface during flotation, therefore, resulting in the large consumption of collectors. Improving collectors’ adsorption degree on the LRC surface and dispersion degree in water [8,9] are of great significance to improve the flotation performance of LRC [10].

Recently, density functional theory (DFT) calculation and molecular dynamics (MD) simulation have been widely used to study the adsorption of collectors on the coal surface [11]. Lu et al. [12] adopted DFT to explore the interactions between hydrocarbon collectors and coal molecules, and the frontier orbital energy gap was found to be in the order of alkanes < olefins < aromatics. Using DFT to calculate the influence of plasma-treated collectors on LRC flotation, Li [13] showed that plasma treatment can improve flotation performance. Ren et al. [14] found that the frontier orbital energy gap and activity of methyl oleate were both higher than those of kerosene, therefore, easily adsorbed onto the coal surface. Liu et al. [15] studied the adsorption behaviors of mixed dodecane/valeric acid collectors on the LRC surface via experiments and MD simulations. The results showed that n-valeric acid could enhance the lipophilicity and hydrophobicity of the LRC surface. Li et al. [16] showed that pyrite oxidation in coal could hinder xanthate adsorption during the flotation separation process through the literatures analyses. Xu et al. [17] studied the effects of the fatty acid unsaturation degree on the LRC flotation. The results showed that the flotation yield of LRC was linolenic acid > linoleic acid > oleic acid > diesel.

Long-flame coal (LFC) is a type of bituminous coal with the lowest degree of metamorphism, and the consumption of conventional flotation collectors is large [18]. Therefore, research on the adsorption of multi-collectors on the LFC surface is of great significance [19].

In the present study, DFT and MD were both adopted to study the adsorption behaviors of a novel synthesis of biodiesel collector (BDC), kerosene, diesel, and diethyl phthalate (DEP) collectors on the LFC surface. Based on the Fourier-transform infrared spectroscopy (FTIR) results, an LFC molecular model was built on the Wisser model, and Gaussian 09 software was used to calculate the molecule's electrostatic potential, the frontier molecular orbital gap, and the binding energy of the LFC and collector. Materials Studio 2018 software was used to calculate the adsorption energy, mean square displacement, correlation density, and coal-collector-water system's radial distribution function, providing references for further developments of new collectors to enhance LRC flotation performance.

2. Materials and Methods

2.1. Functional Groups

Coal samples were obtained from a coal preparation plant in Shanxi. FTIR was used to analyze the oxygen-containing functional groups in the coal sample. After drying, the coal sample was mixed with KBr at a ratio of 1:150, ground to $-2\ \mu\text{m}$, and further pressed into tablets. The sample was tested within the wave number range of $4000\text{--}400\ \text{cm}^{-1}$ [20].

2.2. Molecular Modeling

Due to the complex of LFC molecular structure, LFC molecular fragments and kerosene, diesel, DEP, and BDC molecules were selected for quantum chemistry static simulation. LFC model and the collectors' molecular modeling were completed based on the Wisser model and infrared analyses, respectively. The collectors and LFC molecules before optimization are shown in Figure 1.

2.3. Molecular Electrostatic Potential

Based on B3LYP functional, combined with 6-311G (d, p) basis group and DFT-3D dispersion corrected method, Gaussian 09 software [21] was used to optimize the molecular structure of LFC and collector. Based on m062x functional combined with def2tzvpp basis group and DFT-3D dispersion corrected method, the binding energy between the collector and coal was calculated using Gaussian 09, and the quantum chemistry properties of collectors and LFC were analyzed. Multiwfn 3.8 and VMD [22] were used to plot the molecular surface electrostatic potential of collectors and LFC [23].

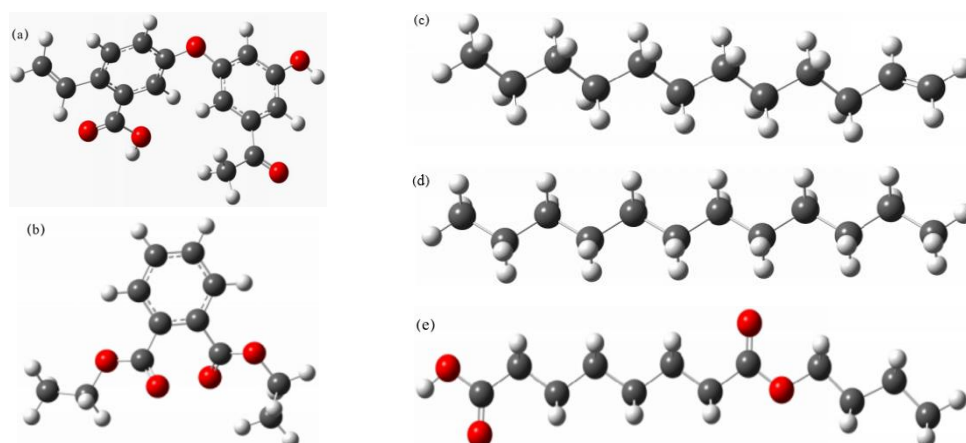


Figure 1. Molecular diagrams before optimization: (a) LFC fragment, (b) DEP, (c) diesel, (d) kerosene, and (e) BDC (Gray balls-carbon atoms, red balls-oxygen atoms, white balls-hydrogen atoms).

2.4. Molecular Frontline Orbitals and Adsorption Energy

In 1951, Kenichi Fukui proposed the frontier molecular orbital theory, which stated that frontier orbitals played a decisive role in chemical reactions [24]. The collector's frontier molecular orbital energy gap was simulated using Gaussian 09 software. The absolute value of the frontier orbital energy gap (E_{GAP}) was used to judge the collector's molecular activity. A smaller absolute value indicates a stronger interaction between collector and coal, thus easing the adsorption of the collector onto LFC surface [25]. The formula of E_{GAP} is as follows:

$$E_{GAP} = E_{LUMO} - E_{HOMO} \quad (1)$$

where E_{HOMO} is the highest occupied molecular orbital energy, eV. E_{LUMO} is the lowest unoccupied molecular orbital energy, eV. E_{GAP} is the frontline orbital energy gap, eV.

Gaussian 09 software was used to calculate the binding energy, which provides an estimate of the stability of collectors during adsorption. The greater the heat released during binding (E_b), the more stable the collector is during adsorption. The formula of E_b is as follows:

$$E_b = E_{c+a} - E_c - E_a \quad (2)$$

where E_{c+a} is the total energy of coal and collector molecules, eV. E_c is the lowest energy of coal after the molecular structure optimization, eV. E_a is the lowest energy of collector after the molecular structure optimization, eV. E_b is the heat released during binding, eV.

2.5. MD Simulation

The Forcite module of Materials Studio 2018 software was used for MD simulation of coal–collector–water systems. With functional GGA-PBE, DNP base group, and fine calculation accuracy, the Dmol 3 module was used to optimize the structure of collector, water, and coal molecules. The dynamic behaviors of water molecules on LFC surface are shown in Figure 2. LFC molecular model was adapted from Wiser coal model, in which 300 water molecules were placed in a $25 \text{ \AA} \times 25 \text{ \AA} \times 14 \text{ \AA}$ cell as the water molecule layer model. Forty coal molecules were placed in a $25 \text{ \AA} \times 25 \text{ \AA} \times 31.7 \text{ \AA}$ cell. Twenty collector molecules were placed in a $25 \text{ \AA} \times 25 \text{ \AA} \times 12.2 \text{ \AA}$ cell, which represented collector surface model. A coal–collector–water molecule system was established through Build Layer, and a 50 \AA vacuum layer was added above the water molecule to eliminate any influence from the Z-direction during the modeling process.

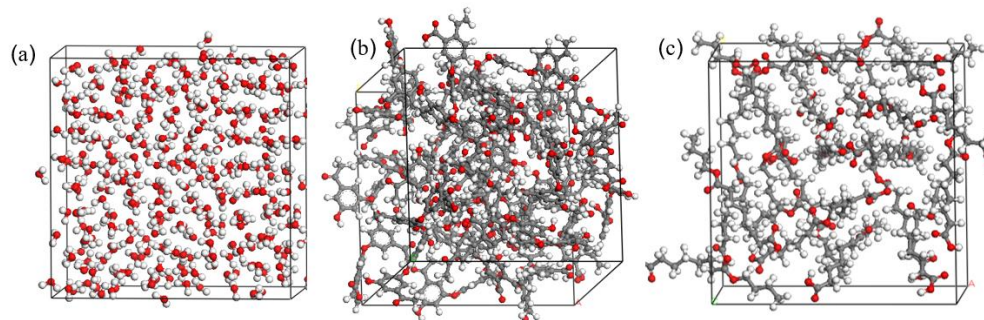


Figure 2. Schematic diagrams of molecular box: (a) water molecule, (b) coal molecule, and (c) BDC molecule (Gray balls-carbon atoms, red balls-oxygen atoms, white balls-hydrogen atoms).

The Forcite module was used to optimize the molecular structure of coal–collector–water system and calculate the system energy. The convergence criterion was defined to fine, and the COMPASS force field was selected. The number of iterations, the energy difference, and the RMS force standard were 50,000, 0.001 kcal/mol, and 0.5 kcal/mol/Å², respectively. The optimized structure was subjected to annealing calculation under 1098 K–298 K, with a calculation step of 5000 and a fine convergence criterion to relax the optimized structure and facilitate subsequent dynamic simulation. The dynamic simulation of the coal–collector–water system was calculated using Forcite module, with a Universal Force Field, a constant particle number, a constant volume and constant temperature (NVT) ensemble, and the Nose temperature control method. The Ewald summation method and atom-based method were selected to calculate the long-range electrostatic interactions and van der Waals interactions, respectively, with a total simulation time of 1 ns.

The interactions between collector and coal surface can be characterized by the total adsorption energy. The larger the total adsorption energy of the system is, the greater the adsorption degree of the collector is. The total adsorption energy of coal–collector–water system is calculated as follows:

$$E = E_{\text{total}} - E_{\text{coal}} - E_{\text{collector}} - E_{\text{water}} \quad (3)$$

where E is the total adsorption energy, eV. E_{total} is the energy of coal–collector–water system, eV. E_{coal} is the energy of coal molecules, eV. $E_{\text{collector}}$ is the energy of collector, eV. E_{water} is the energy of water molecules, eV.

The mean square displacement (MSD) and diffusion coefficient (D), in contrast, explain the influences of collectors on the kinetic properties of water molecules. The equations for MSD and D are as follows:

$$MSD = \frac{1}{N} \sum_{i=1}^N [r_i(t) - r_i(0)]^2 \quad (4)$$

where N is the number of diffusing molecules, $r_i(0)$ is the original position vector of the molecule, $r_i(t)$ is the position vector of the molecule at time t , and t is time.

$$D = \frac{1}{6N} \lim_{t \rightarrow \infty} \frac{d}{dt} \sum_{i=1}^N [r_i(t) - r_i(0)]^2 \quad (5)$$

$$D = \lim_{t \rightarrow \infty} \left(\frac{MSD}{6t} \right) = \frac{1}{6} K_{MSD} \quad (6)$$

where K_{MSD} is the slope of the MSD curve. MSD is the mean square displacement, Å². D is the diffusion coefficient, cm²/s.

The relative density distribution was used to judge the density distribution characteristics of the coal–collector–water system in all directions and analyze the spatial position of the collector, water, and coal and the adsorption state of the collector and water on

the coal surface. The peak value on the relative density distribution curve represents the concentrated position of molecules, groups, or atoms.

The radial distribution function (*RDF*) was used to analyze the relationship between oxygen atoms in BDC and oxygen atoms in coal and determine the number of hydrogen bonds between oxygen atoms in BDC and LFC. The $g(r)$ function in *RDF* represents the probability of finding a particle at a distance r . The calculation formula of $g(r)$ was as follows:

$$g_{i \times r}(r) = \frac{1}{4\pi p_j} \times \frac{dN_{i \times r}}{dr} \quad (7)$$

where p_j is the atomic density, dr is the distance, and $dN_{i \times r}$ is the number of atoms within the range of $r-r + dr$.

3. Results and Discussion

3.1. Functional Groups and Molecular Electrostatic Potential

In 1934, Taggart found that all collectors have polar groups and non-polar groups and preliminarily judged the impact of the molecular structure of collectors on flotation [26]. The hydrophilicity and hydrophobicity of the coal surface were affected by the collectors' hydrocarbon chain length, and the adsorption of the collector on the coal surface was affected by the collectors' functional groups.

The infrared spectra of LFC and collectors are shown in Figure 3. LFC exhibited stretching vibration peaks of -OH at 3696 cm^{-1} , 3621 cm^{-1} , 3429 cm^{-1} , and 914 cm^{-1} . The stretching vibration absorption peaks of C-H on fatty hydrocarbons and cycloalkanes were located at 2922 cm^{-1} and 2849 cm^{-1} . The stretching vibration peak of C=O appeared at 1617 cm^{-1} , indicating that the coal sample contains aldehydes, ketones, etc. A stretching vibration peak of COO- appeared at 1436 cm^{-1} . The stretching vibration peak of C-O-C appeared at 1033 cm^{-1} , 779 cm^{-1} , and 691 cm^{-1} , which were mainly C-H structures on aromatic hydrocarbons. In addition, $670\text{--}860 \text{ cm}^{-1}$ was out of the plane bending vibration absorption peak of benzene ring =CH. BDC contained oxygen-containing functional groups (-COOH and -COOR), and LFC was observed to be rich in oxygen-containing functional groups (-COOH, -OH, C-O-C, and C=O), with a C atom content of 55.82%.

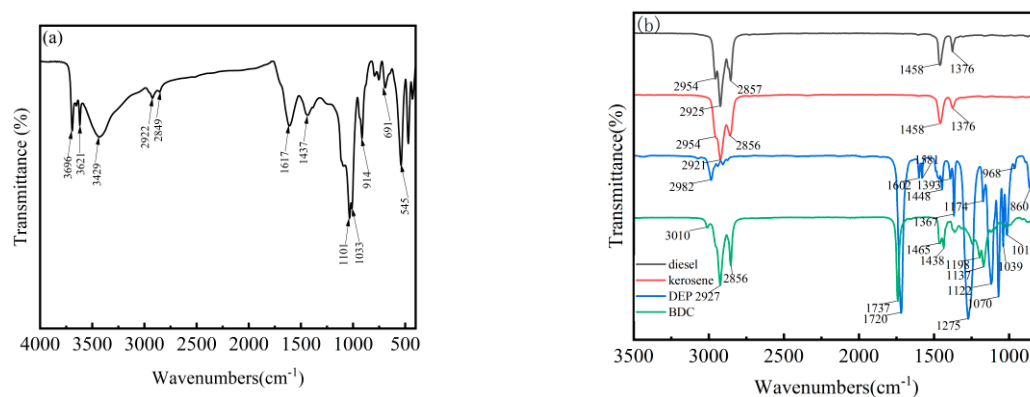


Figure 3. Infrared spectrum: (a) LFC, (b) diesel, kerosene, DEP, and BDC.

The electrostatic potential is well-applicable in qualitative analysis and could be used to predict the active site on the molecular surface. A comprehensive study of the collector adsorption configuration will be helpful for deeper understanding of the interaction between the collector and coal. The electrostatic potential can be used to predict the active site on the molecular surface [27]. The depth of the color represents the positive and negative electrostatic potential around the atom, with red indicating a positive value and blue indicating a negative value. The molecular electrostatic potential diagrams of the collectors are shown in Figure 4. The golden and blue balls represent the maximum and minimum points of the electrostatic potential, respectively. The maximum electrostatic potential around the

O atom in BDC was -0.49 eV, with strong interactions from positively charged particles. The maximum electrostatic potential around the C and H atoms was 0.62 eV and 0.26 eV, respectively, with strong interactions from negatively charged particles.

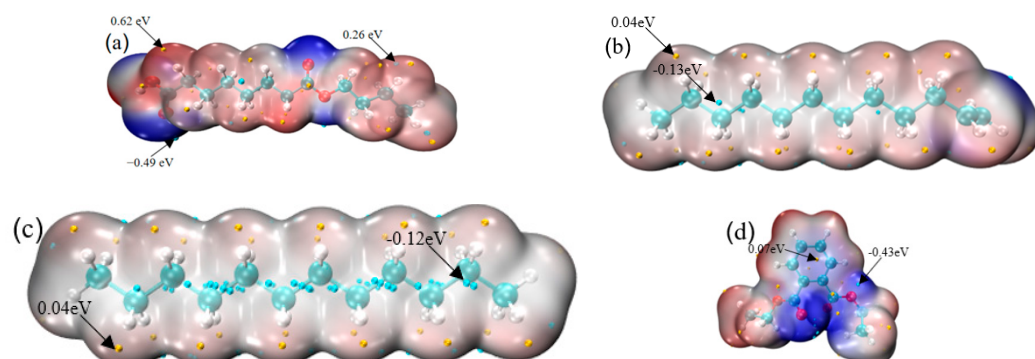


Figure 4. The electrostatic potential diagrams of collectors: (a) BDC, (b) diesel, (c) kerosene, and (d) DEP (Cyan balls-carbon atoms, red balls-oxygen atoms, white balls-hydrogen atoms).

The electrostatic interaction between the collector and coal can determine the functional groups and adsorption sites. Figure 5 shows the electrostatic interaction between collectors and coal. (Blue indicates that the electronegativity was negative and electrons were obtained during the electrostatic interaction. Red indicates that the electronegativity was positive, in which electrons were lost during the electrostatic interaction.) During the electrostatic interaction, kerosene adsorbed carbonyl and hydroxyl groups in coal, diesel adsorbed carboxyl and hydroxyl groups in coal, DEP adsorbed carboxyl groups in coal, and BDC bidirectionally adsorbed carboxyl groups in coal.

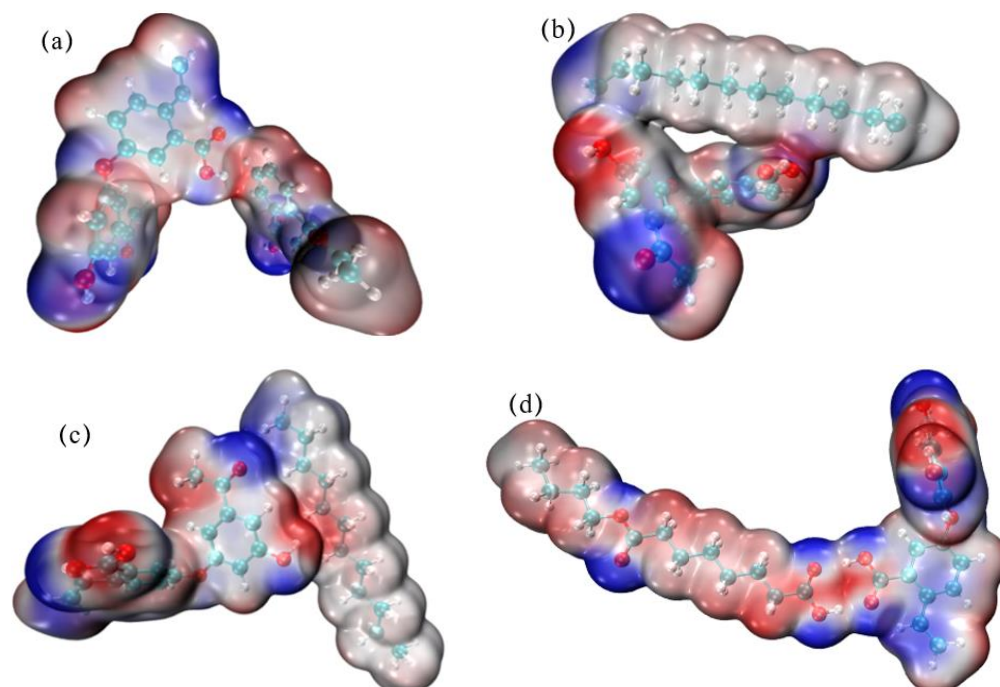


Figure 5. The electrostatic interaction diagrams of collectors with coal: (a) DEP, (b) diesel, (c) kerosene, and (d) BDC (Cyan balls-carbon atoms, red balls-oxygen atoms, white balls-hydrogen atoms).

3.2. Molecular Frontline Orbits and Adsorption Energy

The frontier molecular orbitals are shown in Table 1. Although having the same carbon atom number, the E_{LUMO} , E_{HOMO} , and E_{GAP} of all four collectors were observed to

be different. Additionally, the order of chemical reaction activity, E_{GAP} , was BDC > DEP > diesel > kerosene.

Table 1. The frontier molecular orbitals of collectors (eV).

Names	E_{LOMO}	E_{HOMO}	E_{GAP}
Kerosene	0.09	−0.29	0.38
Diesel	0.03	−0.25	0.28
DEP	0.01	−0.26	0.27
BDC	−0.05	−0.25	0.20

Hydrogen bonds were formed between oxygen-containing functional groups on the LFC surface and oxygen-containing functional groups on the surface of collectors. In addition, hydrogen bonds can be formed between coal and water. Hydrogen bonding was used to determine the adsorption strength of collectors and water on the coal surface. The hydrogen bonds among BDC, water molecules, and coal molecules are shown in Figure 6. During the adsorption of the collector and LFC molecule, hydrogen bonds were not formed among kerosene, diesel, and DEP and the LFC surface, while they formed between BDC and the LFC surface. The O and H atoms in the carboxyl group of the LFC surface and in the carboxyl group of BDC were bidirectionally adsorbed. Two hydrogen bonds with lengths of 1.70 Å were formed between BDC and the carboxyl groups of LFC. Additionally, two hydrogen bonds with lengths of 1.73 Å and 1.93 Å were formed between water and the carboxyl groups of LFC, respectively. The former hydrogen bonds were shorter and stronger than the latter, while BDC molecules replaced the adsorption sites of water molecules on the LFC surface.

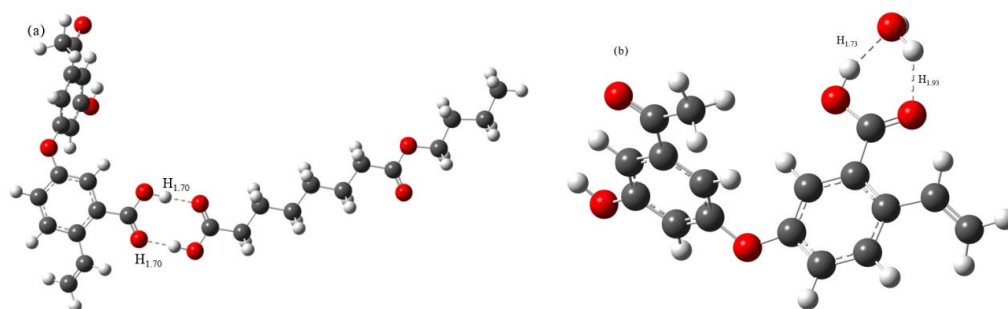


Figure 6. The hydrogen bond interactions among BDC, water, and coal molecules: (a) BDC molecules and (b) water molecules (Gray balls-carbon atoms, red balls-oxygen atoms, white balls-hydrogen atoms).

The binding energy of collectors and coal molecules is shown in Table 2. The minimum energy was −9.03 eV. When the collector interacted with LFC in static electricity, kerosene adsorbed carbonyl and hydroxyl groups in LFC and the diesel adsorbed carboxyl and hydroxyl groups in LFC, DEP adsorbed carboxyl groups in LFC, and BDC bidirectionally adsorbed carboxyl groups in LFC. The order of binding energy was observed to be BDC > DEP > diesel > kerosene, whereby BDC adsorption was relatively stable.

Table 2. The binding energy of collectors and coal molecules (eV).

Names	E_c	E_a	E_{c+a}	E_b
Kerosene	−1032.35	−472.88	−1505.77	−0.54
Diesel	−1032.35	−471.66	−1504.56	−0.55
DEP	−1032.35	−766.62	−1799.54	−0.57
BDC	−1032.35	−771.44	−1804.40	−0.61

3.3. MD Simulation

Sorbitan oleate (Span 80) and Polysorbate (Tween 80) were used to emulsify BDC. The mixing ratio of emulsifiers was 9.35% for Span-80 (HLB = 4.3) and 90.65% for Tween-80 (HLB = 15.0).

The energy and total adsorption energy of the coal–collector–water system are shown in Table 3. In the coal–collector–water system, the total adsorption energy of emulsified BDC (EBDC) was, interestingly, negative at -39.41 eV. The higher the absolute value of the total adsorption energy was, the higher the adsorption energy and adsorption degree was. The adsorption energy of EBDC was higher than that of BDC. Emulsifiers can improve the molecular force and adsorption of BDC and LFC, thereby strengthening flotation performance.

Table 3. The energy and total adsorption energy of coal–collector–water system (eV).

Names	E_{coal}	E_{water}	$E_{\text{collector}}$	E_{total}	E
Kerosene	-3638.75	-3445.50	-611.07	-7715.99	-20.67
Diesel	-3638.75	-3445.50	-775.80	-7890.30	-30.25
DEP	-3638.75	-3445.50	585.62	-6530.90	-32.27
BDC	-3638.75	-3445.50	-1461.79	-8581.49	-35.45
EBDC	-3638.75	-3445.50	-866.87	-7990.53	-39.41

Figure 7 shows the dynamic simulation process of the coal–collector–water molecular system. In this system, LFC was located below, the collector was in the middle, and the water molecules were located above. For coal–kerosene and diesel–water molecular systems, water molecules gradually spread and diffused onto the LFC surface, and the collector was dispersed onto the LFC surface under the weak interactions between water and collector molecules. The hydrogen bonds, however, were not formed on the LFC surface. The collector only interacted with the LFC surface, and the adsorption degree was relatively small. For the coal–DEP–water molecular system, DEP formed hydrogen bonds with water molecules, interacted deeper into the LFC layers with a higher adsorption degree, and showed poor dispersion on the LFC surface. Water molecules, however, did not laterally diffuse on the LFC surface. For the coal–BDC–water molecular system, water molecules laterally diffused across the LFC surface. Due to the weak interactions between water and collectors, the collectors dispersed onto the LFC surface, forming hydrogen bonds on the LFC surface. The collectors interacted with both the LFC surface and deep layers, and the adsorption degree was large. For the coal–EBDC–water molecular system, emulsifiers adsorbed at the oil–water interface, and BDC was observed to be more compacted on the LFC surface, thus improving the dispersion and adsorption degrees of the collector on the LFC surface.

3.4. Mean Square Displacement

The mean square displacement (MSD) and the diffusion coefficient (D) can explain the effects of different collectors on the diffusion of the water molecules and the hydrophobicity of the coal surface. Figure 8 shows the mean square displacement (MSD) of five collectors' molecular systems. The diffusion coefficient (D) is one-sixth of the slope of the image. In the systems of kerosene, diesel, DEP, BDC, and EBDC, the D of water molecules was 3.61×10^{-5} cm²/s, 6.66×10^{-5} cm²/s, 1.19×10^{-4} cm²/s, 2.83×10^{-4} cm²/s, and 3.73×10^{-4} cm²/s, respectively. The D of water molecules in EBDC was observed to be the highest, thus suggesting that the emulsifier enhanced the lipophilicity and hydrophobicity of the LFC surface, slowed down the diffusion of BDC on the LFC surface, and accelerated the speed of water molecules leaving the LFC surface.

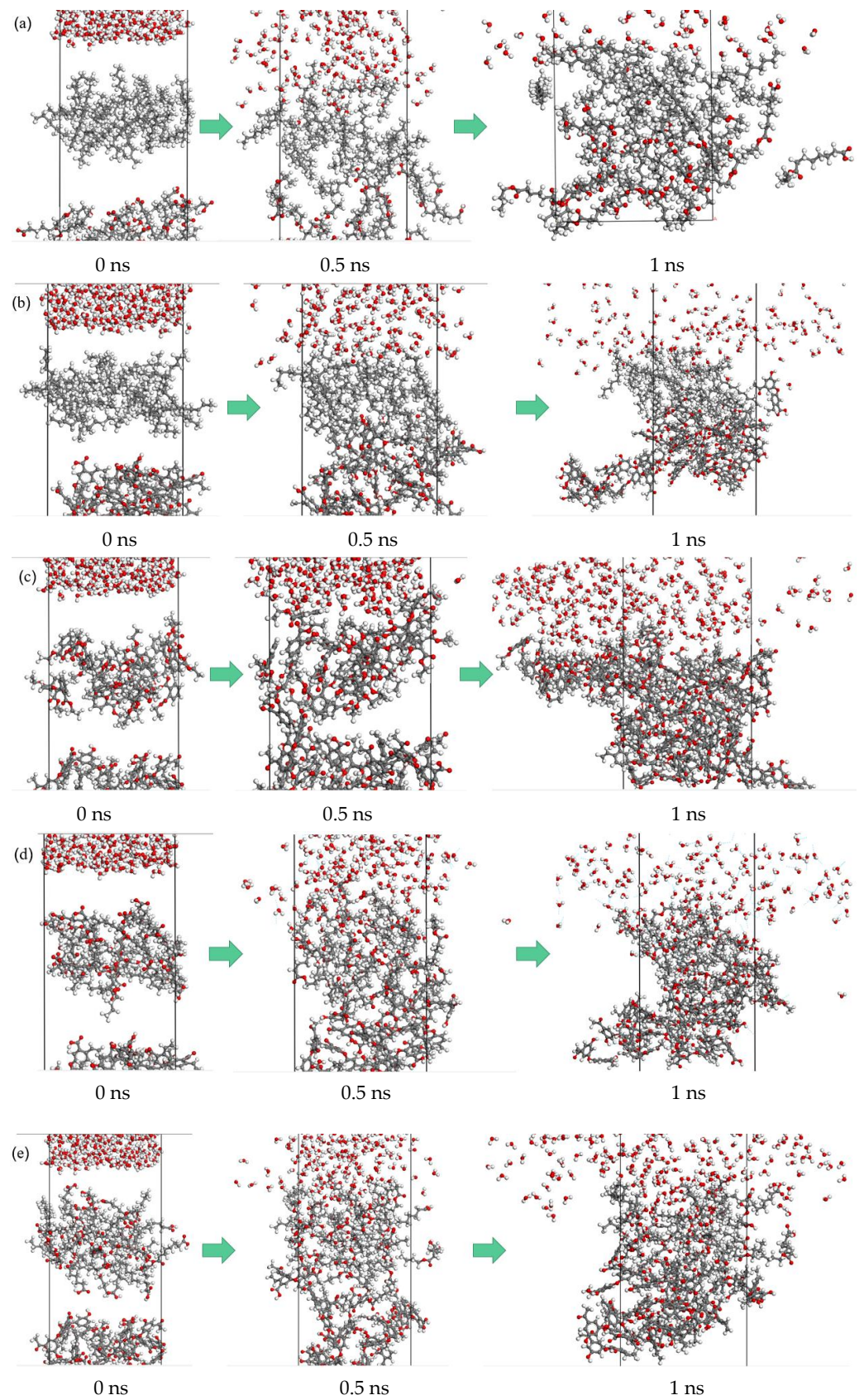


Figure 7. The dynamics simulation process of coal-collector-water molecular system: (a) kerosene, (b) diesel, (c) DEP, (d) BDC, and (e) EBDC. (Gray balls-carbon atoms, red balls-oxygen atoms, white balls-hydrogen atoms).

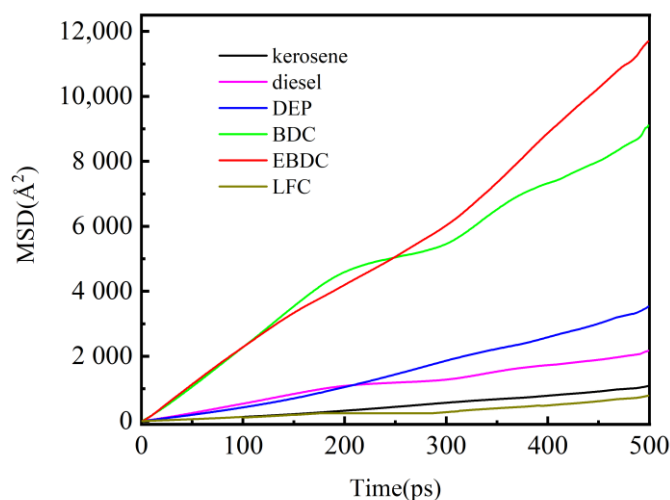


Figure 8. MSD curves of collector molecules on water molecules of LFC surface.

3.5. Relative Density and RDF

The relative concentration distribution can effectively assist in studying the adsorption morphology of collectors on the coal surface and determining the collectors' adsorption degree during the flotation process. The relative density distribution of five collector molecules (kerosene, diesel, DEP, BDC, and EBDC), water, and coal, in the vertical direction, was shown in Figure 9. Figure 9a showed the distribution of water molecules was 10–45 Å, that of kerosene molecules was 32.5–57.5 Å, and that of peaks was 42.5–47.5 Å. The peak values of water molecules were concentrated at 55.5–62.5 Å, and the distribution of kerosene molecules and water molecules was uniformed. The kerosene molecules at the peak position replaced the adsorption sites of water molecules on the LFC surface. In Figure 9b, the peak values of diesel molecules were concentrated at 37–45 Å, those of water molecules were mainly concentrated at 40–90 Å, and those of peaks were observed to be scattered at 52–90 Å. Due to the weak interaction between carbon–carbon double bonds and water molecules in diesel molecules, the distribution of diesel and water molecules was uneven. In Figure 9c, coal molecules are distributed at 0–45.5 Å, DEP has peaks at 40 Å and 45 Å, water molecules have peaks at 11 Å and 55 Å, and DEP molecules mainly adsorb coal molecules at 40–45 Å. The diffusion degree of water molecules on the LFC surface was small, and the DEP dispersion in slurry was suggested to be poor. In Figure 9d, the peak values of water molecules are uniformly distributed between 55 and 65 Å, and the peak values of BDC are higher than those of water molecules. BDC molecules at positions 40 to 50 Å replaced the adsorption sites of water molecules on the coal molecules' surface. In Figure 9e, the emulsifier was observed to be adsorbed at the oil–water interface of the coal–collector–water system. DEP acted on the long-flame coal surface, while BDC acted on the deep layer of LFC. The overlap area between EBDC and coal molecules was noted to be greater than that of BDC and coal molecules, indicating that the adsorption strength of EBDC was greater than that of BDC. The emulsifier made BDC more compact and distributed on the LFC surface, increasing the BDC dispersion degree during flotation. Finally, in Figure 9f, the peak intensity of RDF between the O atom in LFC and the O atom in EBDC is higher than the peak intensity of RDF between the O atom in LFC and the O atom in BDC before emulsification. The presence of an emulsifier not only increased the number of hydrogen bonds between the BDC molecule and oxygen-containing functional groups on the LFC surface, making BDC more closely adsorbed on the LFC surface and also increasing the BDC adsorption degree on the LFC surface.

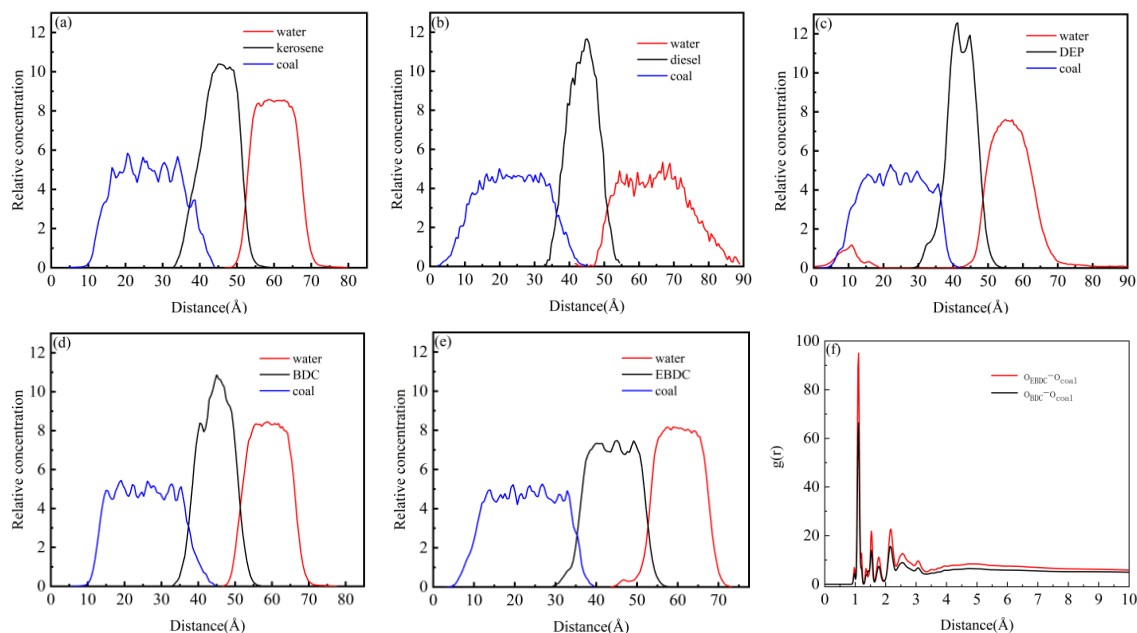


Figure 9. Relative concentration distribution diagrams: (a) kerosene, (b) diesel, (c) DEP, (d) BDC, (e) EBDC, and (f) RDF.

4. Conclusions

- Electrostatic interaction and hydrogen bonding are the basis for determining the adsorption degree between collectors and LFC. When the collector interacted with LFC in static electricity, kerosene adsorbed carbonyl and hydroxyl groups in LFC, diesel adsorbed carboxyl and hydroxyl groups in LFC, DEP adsorbed carboxyl groups in LFC, and BDC bidirectionally adsorbed carboxyl groups. The bond length of hydrogen bonds between BDC molecules and LFC was shorter than that between water molecules and LFC. The interaction between BDC and LFC was stronger than that between water and LFC. BDC molecules replaced the adsorption sites of water molecules on the LFC surface, and hydrogen bonding increased the BDC adsorption degree on the LFC surface. Based on the adsorption energy and E_{GAP} criteria, the reaction activity and stability of the collector, as well as the order of adsorption energy, were observed as follows: BDC > DEP > diesel > kerosene. The diffusion coefficients of water molecules in the five collectors (EBDC, BDC, DEP, diesel, and kerosene) were calculated to be $3.73 \times 10^{-4} \text{ cm}^2/\text{s}$, $2.83 \times 10^{-4} \text{ cm}^2/\text{s}$, $1.19 \times 10^{-4} \text{ cm}^2/\text{s}$, $6.66 \times 10^{-5} \text{ cm}^2/\text{s}$, and $3.61 \times 10^{-5} \text{ cm}^2/\text{s}$. The emulsifier increased the diffusion coefficient of water molecules in the collector system, slowed down the diffusion of BDC on the LFC surface, and accelerated the speed of water molecules leaving the LFC surface.
- The emulsifier adsorbed at the oil–water interface of the coal–BDC–water system, thus promoting a decrease in the contact area between the collector and water molecules and an increase in the contact area between the collector and coal molecules. The emulsifier increased the probability of O atoms appearing around the O atoms in BDC and the number of hydrogen bonds between BDC and LFC, thereby improving the dispersion of BDC during flotation.

Author Contributions: G.C.: conceptualization, methodology, formal analysis, investigation, resources, writing—review and editing, supervision, project administration, and funding acquisition. Y.P.: software, validation, formal analysis, investigation, data curation, and writing—original draft. Y.L.: conceptualization, methodology, supervision, and funding acquisition. M.Z.: resources and writing—review and editing. All authors have read and agreed to the published version of the manuscript.

Funding: This research was funded by the “Foundation for University Key Teacher by Henan Province” (grant no. 2020GGJS051); the “Key Scientific and Technological Project of Henan Province” (grant no. 232102321134, 222102320284); the “Open Foundation of State Environmental Protection Key Laboratory of Mineral Metallurgical Resources Utilization and Pollution Control” (grant no. HB202201); the “Research Fund of Henan Key Laboratory for Green and Efficient Mining & Comprehensive Utilization of Mineral Resources (Henan Polytechnic University)” (grant no. KCF2213); the “College Students’ Innovative Entrepreneurial Training Plan Program” (grant no. 202310460076); and the “Henan Polytechnic University Science Fund for Distinguished Young Scholars” (grant no. J2021-1).

Data Availability Statement: Not applicable.

Conflicts of Interest: The authors declare no conflict of interest.

Abbreviations

BDC	Biodiesel collector
DEP	Diethyl phthalate
DFT	Density functional theory
EBDC	Emulsified biodiesel collector
FTIR	Fourier-transform infrared spectroscopy
LFC	Long-flame coal
LRC	Low-rank coal
MD	Molecular dynamics
MSD	Mean square displacement
RDF	Radial distribution function

References

1. Wu, X.; Qin, Z.; Yang, X.; Lin, Z. Advances in the modification of coal-based porous carbon for supercapacitors. *Clean Coal Technol.* **2022**, *28*, 94–102.
2. Yu, Y.; Liu, J.; Jia, X.; Min, C.; Liu, F.; Zhang, N.; Chen, S.; Zhu, Z.; Zhou, A. A New Perspective on the Understanding of High-Intensity Conditioning: Incompatibility of Conditions Required for Coarse and Fine Coal Particles. *Min. Proc. Ext. Met. Rev.* **2022**, 1–10. [[CrossRef](#)]
3. Mao, Y.; Xia, W.; Peng, Y.; Xie, G. Dynamic pore wetting and its effects on porous particle flotation: A review. *Int. J. Min. Sci. Technol.* **2022**, *32*, 1365–1378. [[CrossRef](#)]
4. Li, M.; Xing, Y.; Zhu, C.; Liu, Q.; Yang, Z.; Zhang, R.; Zhang, Y.; Xia, Y.; Gui, X. Effect of roughness on wettability and floatability: Based on wetting film drainage between bubbles and solid surfaces. *Int. J. Min. Sci. Technol.* **2022**, *32*, 1389–1396. [[CrossRef](#)]
5. Xia, Y.; Zhang, R.; Cao, Y.; Xing, Y.; Gui, X. Role of molecular simulation in understanding the mechanism of low-rank coal flotation: A review. *Fuel* **2020**, *262*, 116535. [[CrossRef](#)]
6. Xia, Y.; Zhang, R.; Xing, Y.; Gui, X. Improving the adsorption of oily collector on the surface of low-rank coal during flotation using a cationic surfactant: An experimental and molecular dynamics simulation study. *Fuel* **2019**, *235*, 687–695. [[CrossRef](#)]
7. Cheng, G.; Li, Y.; Zhang, M. Research progress on desulfurization technology of high-sulfur bauxite. *Trans. Nonferrous Metal. Soc.* **2022**, *32*, 3374–3387. [[CrossRef](#)]
8. Zheng, K.; Zhang, W.; Li, Y. Enhancing flotation removal of unburned carbon from fly ash by coal tar-based collector: Experiment and simulation. *Fuel* **2023**, *332*, 126023. [[CrossRef](#)]
9. Wang, S.; Xia, Q.; Xu, F. Investigation of collector mixtures on the flotation dynamics of low-rank coal. *Fuel* **2022**, *327*, 125171. [[CrossRef](#)]
10. Cheng, G.; Zhang, M.; Zhang, Y.; Lin, B.; Zhan, H.; Zhang, H. A novel renewable collector from waste fried oil and its application in coal combustion residuals decarbonization. *Fuel* **2022**, *323*, 124388. [[CrossRef](#)]
11. Cheng, G.; Li, Y.; Zhang, M.; Cao, Y. Simulation of the adsorption behavior of CO₂/N₂/O₂ and H₂O molecules in lignite. *J. China Coal Soc.* **2021**, *46*, 960–969. [[CrossRef](#)]
12. Lu, T.; Li, Z.; Liu, A.; Zhang, Z.; Fan, M. Quantum chemistry calculation of the performance of hydrocarbon flotation reagents. *China Coal* **2015**, *41*, 84–87.

13. Li, W. *Study on the Flotation Reagents Treated by Plasma to Enhance Low-Rank Coal flotation*; China University of Mining and Technology: Xuzhou, China, 2022; pp. 44–48.
14. Ren, C.; Li, Z.; Liu, A.; Liu, Y.; Fan, M. Capture performance and quantum chemistry calculation of methyl oleate on long flame coal surface. *Coal Sci. Technol.* **2020**, *48*, 197–202.
15. Liu, Z.; Xia, Y.; Lai, Q.; An, M.; Liao, Y.; Wang, Y. Adsorption behavior of mixed dodecane/n-valeric acid collectors on low-rank coal surface: Experimental and molecular dynamics simulation study. *Colloid. Surf. A* **2019**, *583*, 123840. [[CrossRef](#)]
16. Li, Y.; Cheng, G.; Zhang, M.; Cao, Y.; Lau, E. Advances in depressants used for pyrite flotation separation from coal/minerals. *Int. J. Coal. Sci. Technol.* **2022**, *9*, 54. [[CrossRef](#)]
17. Xu, M.; He, L.; Si, W.; Bao, X.; Liu, X.; Xing, Y.; Gui, X.; Cao, Y. Influence mechanism of fatty acid unsaturation on the intensification of low-rank coal flotation. *China J. Eng.* **2023**, *45*, 195–205.
18. Zhang, M.; Cheng, G.; Lu, Y.; Cao, Y.; Lau, E. Preparation of long-flame coal flotation collector from waste cooking oil. *Miner. Eng.* **2023**, *202*, 108296. [[CrossRef](#)]
19. Li, E.; Lu, Y.; Cheng, F.; Wang, X.; Miller, J. Effect of oxidation on the wetting of coal surfaces by water: Experimental and molecular dynamics simulation studies. *Physicochem. Probl. Miner. Process.* **2018**, *54*, 1039–1051.
20. Cheng, G.; Li, Y.; Cao, Y.; Zhang, Z. A novel method for the desulfurization of medium-high sulfur coking coal. *Fuel* **2023**, *335*, 126988. [[CrossRef](#)]
21. Frisch, A. *Gaussian 09W Reference*; Gaussian, Inc.: Wallingford, CT, USA, 2009; pp. 3–14.
22. VMD-Visual Molecular Dynamics. Available online: <https://www.ks.uiuc.edu/Research/vmd/> (accessed on 1 September 2023).
23. Lu, T.; Chen, F. Multiwfn: A multifunctional wavefunction analyzer. *J. Comput. Chem.* **2012**, *33*, 580–592. [[CrossRef](#)]
24. Kang, W.; Ma, Z. Physical and chemical properties of coal pyrite and flotation desulfurization. *Clean Coal Technol.* **2022**, *28*, 109–117.
25. Cheng, G.; Zhang, J.; Su, H.; Zhang, Z. Synthesis and Characterization of a Novel Collector for the Desulfurization of Fine High-sulfur Bauxite via Reverse Flotation. *Particuology* **2023**, *79*, 64–77. [[CrossRef](#)]
26. Chen, J. Structure and mechanism of flotation collectors. *Conserv. Util. Miner. Resour.* **2017**, *4*, 98–106.
27. Lu, T.; Chen, F. Quantitative analysis of molecular surface based on improved Marching Tetrahedra algorithm. *J. Mol. Graph. Model.* **2012**, *38*, 314–323. [[CrossRef](#)] [[PubMed](#)]

Disclaimer/Publisher’s Note: The statements, opinions and data contained in all publications are solely those of the individual author(s) and contributor(s) and not of MDPI and/or the editor(s). MDPI and/or the editor(s) disclaim responsibility for any injury to people or property resulting from any ideas, methods, instructions or products referred to in the content.